

# Grain-size dependence of the mechanical properties of an age-hardening Fe-1 % Cu-alloy

E. HORNBOGEN, G. STANIEK\*

*Institut für Werkstoffe, Ruhr-Universität Bochum, 463 Bochum, Germany*

The contribution of grain size and precipitation hardening to the yield stress and other mechanical properties was investigated. An alloy of iron with 1% copper was prepared as supersaturated solid solution with grain sizes between 12 and 140  $\mu\text{m}$ . By ageing at 500 and 600°C different precipitation hardening conditions were produced.

For small particle sizes an additive behaviour of grain-boundary and precipitation hardening was found (particle radius  $r < 50 \text{ \AA}$ ). For large particle sizes the yield stress is independent of grain size ( $r > 150 \text{ \AA}$ ). A transition is found for intermediate particle sizes with grain size dependence for small and independence for large grain sizes ( $50 \text{ \AA} < r < 150 \text{ \AA}$ ).

The effect of grain boundaries and particles on the formation and motion of dislocations is used to explain this behaviour.

## List of symbols

$\sigma_y$ ,	measured yield stress
$\Delta\sigma$ ,	increase in yield stress
$\Delta\sigma_p$	particle hardening
$\Delta\sigma_b$ ,	grain-boundary hardening
$\Delta\sigma_s$ ,	solid solution hardening
$\sigma_{\alpha\text{-Fe}}$ ,	yield stress of a pure $\alpha$ -Fe crystal
$\sigma_0$ ,	yield stress of the alloy at $D^{-1/2} = 0 \equiv D = \infty$
$D$ ,	grain size
$k_y$ ,	slope of Hall-Petch-relation
$\mathbf{b}$ ,	Burgers vector
$\epsilon$ ,	plastic strain
$\rho_y$ ,	dislocation density at 0.2% strain
$\rho_b$ ,	density of dislocation generated at grain boundaries
$\rho_s$ ,	dislocation density from second sources
$\rho_p$ ,	density of dislocations generated at particles
$\lambda$ ,	average free path of dislocation
$G$ ,	shear modulus
$\alpha$ ,	constant factor relating $\Delta\sigma$ and $\rho$
$\sigma_u$	ultimate tensile strength

## 1. Introduction

The increase in the yield stress of metals due to

individual hardening mechanisms has been discussed previously [1]. Quantitative relationships between the increase in yield stress and the concentration of certain obstacles can be obtained. Little is known, however, on the combination of elementary hardening mechanisms, especially on quantitative relationships between the contributions due to more than one mechanism [2-4]. The interaction of one dislocation with mixtures of obstacles has been discussed theoretically [5]. Precipitation hardening and hardening due to grain boundaries are two important elementary hardening mechanisms, the combination of which has not yet quantitatively been investigated. It cannot be treated by the formulae given by Foreman and Makin [5] because the interpretation of grain-size dependence of yield stress requires consideration of an interaction of more than one dislocation with a grain boundary. An iron-copper-alloy was used as a model alloy for this investigation. It was chosen because its precipitation behaviour is well known and relatively simple [6]. Only two phases and no intermetallic compounds occur, and treatments that produce different grain sizes and different

\*Present address: Department Metaalkunde, Katholieke Universiteit Leuven, G. de Croylaan 2, 3030 Heverlee, Belgium.

precipitation conditions can be performed independently in different temperature ranges. The precipitation kinetics are relatively simple. At the beginning of ageing, copper-rich bcc coherent zones form in the  $\alpha$ -iron matrix. Above a radius of about 30 to 40 Å these zones start to transform into the fcc structure and lose simultaneously their coherency. Consequently, only particle growth occurs.

## 2. Experimental methods

The main objective of the experimental work was

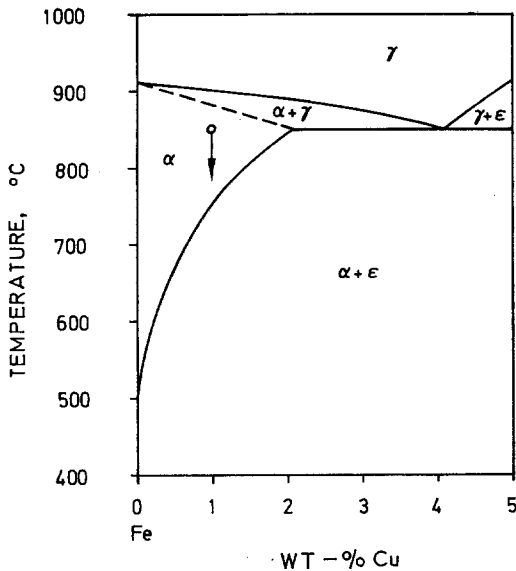


Figure 1 The equilibrium diagram of the Fe—Cu—System [7].

to measure the mechanical properties, especially the yield stress, for various grain sizes and precipitation conditions.

The material had the following composition: 1.000% Cu, 0.006% C, 0.002% N, balance Fe. Sheets 5 mm thick were produced by forging, hot-rolling, cold-rolling and grinding. The heat-treatment temperatures are indicated in Fig. 1 [7]. Different grain sizes were produced by cold-rolling or stretching of tensile specimens, followed by recrystallization at 850°C. Homogeneous solid solutions are obtained with a grain size range between 12 and 140  $\mu\text{m}$ .

Precipitation of copper was obtained by ageing treatments between 500 and 600°C for 1 to 100 h. In this way particles with a maximum radius of 160 Å were produced.

Mechanical measurements were conducted with sheet tensile tests and sheets of 100 mm length and 5 to 20 mm<sup>2</sup> cross-sectional area. In each case the thickness of the sheet was more than ten times the grain diameter.

Some of the specimens were tested until rupture, others were deformed to a defined amount of plastic strain in order to obtain deformed specimens for electron microscopy. The microstructure was determined by transmission electron microscopy of thin foils and replicas, while light microscopy was used for grain size determination. Transmission electron microscopy was especially suited for the investigation of the nature of the particles and the interaction of dislocations with particles. The

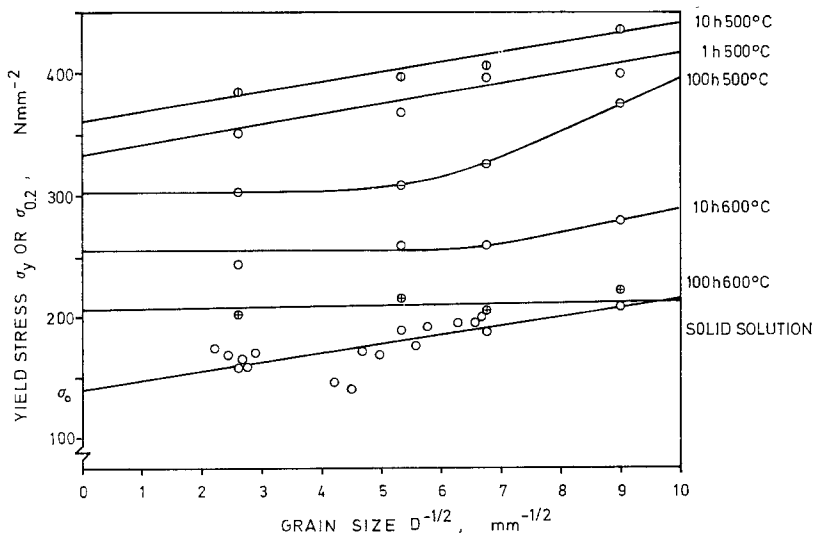


Figure 2 Grain-size dependence of the yield stress of an  $\alpha$ -Fe—1% Cu alloy in different precipitation conditions.

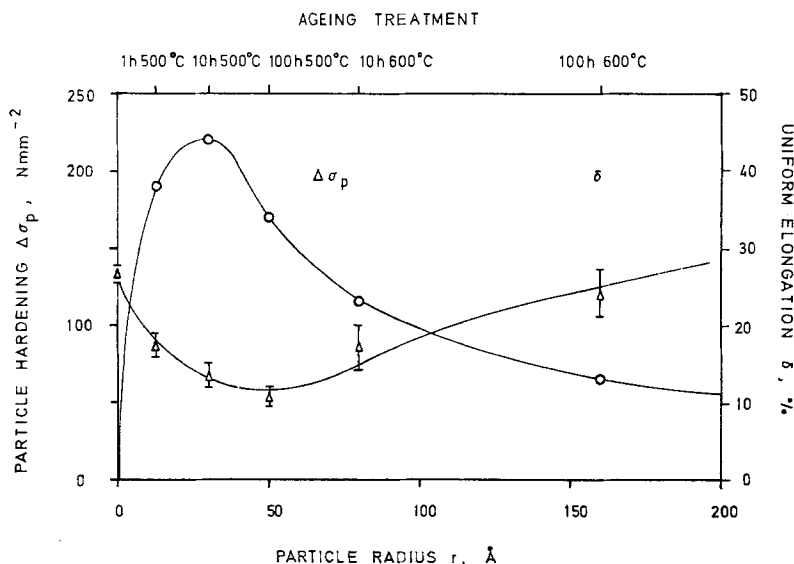


Figure 3 Increase in yield stress due to particle hardening and uniform elongation as a function of particle radius.

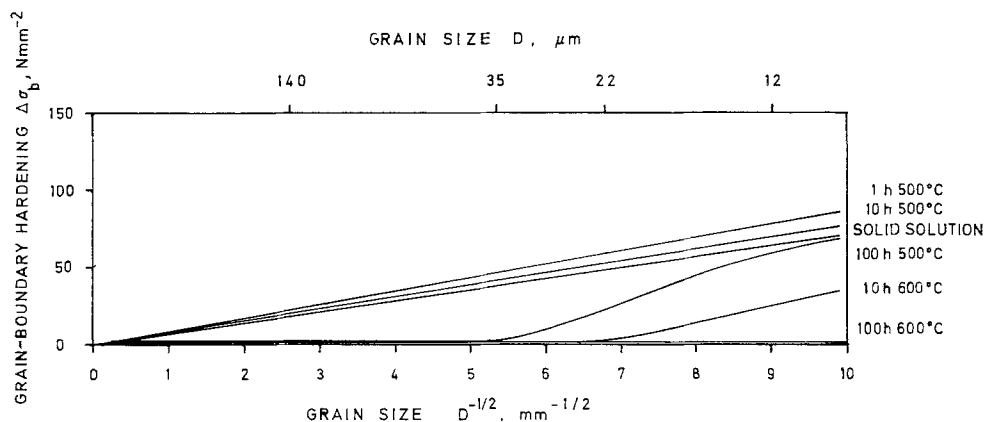


Figure 4 Increase in yield stress by grain-boundary hardening as a function of (grain size)<sup>-1/2</sup>.

replica method led to quantitative data on particle diameters and spacings.

### 3. Experimental results

#### 3.1. Mechanical properties

The results of the yield stress measurements are summarized in Fig. 2. The grain-size dependence of yield stress is plotted for various ageing treatments. For the analysis of the results, the different contributions to the yield stress have to be separated. This can be done according to the following scheme:

$$\sigma_y = \sigma_{\alpha\text{-Fe}} + \Delta\sigma_s + \Delta\sigma_p + \Delta\sigma_b \quad (1)$$

where  $\sigma_{\alpha\text{-Fe}}$  = yield stress of the pure iron matrix;  $\Delta\sigma_s$  = increase due to solid solution hardening;  $\Delta\sigma_p$  = contribution due to particle

hardening;  $\Delta\sigma_b$  = grain-boundary hardening.

The contribution  $\sigma_{\alpha\text{-Fe}} + \Delta\sigma_s \approx 140 \text{ N mm}^{-2}$  is assumed to be constant. The increase in yield stress  $\Delta\sigma$  with which this paper is concerned is due to particle and grain-boundary hardening:

$$\Delta\sigma = \Delta\sigma_p + \Delta\sigma_b \quad (2)$$

The contribution of the individual hardening mechanisms are not simply additive and independent of each other. The subject of the present paper will be to show the special dependence of  $\Delta\sigma_p$  and  $\Delta\sigma_b$ .

From Fig. 2, it follows that the contribution of particle hardening is:

$$\begin{aligned} \Delta\sigma_p &= \sigma_y(D^{-1/2} = 0) - \sigma_{\alpha\text{-Fe}} - \Delta\sigma_s \\ &= \sigma_0 - \sigma_{\alpha\text{-Fe}} - \Delta\sigma_s \end{aligned} \quad (3)$$

In Fig. 3 the particle hardening,  $\Delta\sigma_p$ , is shown as a function of the average radius of the copper particles. The particle size at which maximum yield stress occurs is identical with the transition from shearing to bypassing of particles [8]. If an increasing number of particles are bypassed, the value of  $\Delta\sigma_p$  approaches that which is expected from the Orowan equation [9].

After the contribution of precipitation hardening has been eliminated from the data given in Fig. 2, a grain-size dependence of the yield stress is left, which is indicated in Fig. 4. The grain-size dependence of yield stress is dependent on the precipitation condition. Three different ranges can be distinguished:

1. The homogeneous solution and the ageing conditions where particles are sheared (particle radius  $r < 50 \text{ \AA}$ ): the Petch-Hall-relationship [10] is obtained and grain-boundary hardening occurs to the same absolute amount in solid solutions and precipitation hardened alloys:

$$\Delta\sigma_b = \Delta\sigma_{b \max} = k_y D^{-1/2}. \quad (4)$$

2. Medium particle sizes ( $50 \text{ \AA} < r < 150 \text{ \AA}$ ): there is a transition range for medium particle sizes in which there is a grain-size dependence of yield stress for small grain sizes while it becomes independent for large ones:

$$\Delta\sigma_b < k_y D^{-1/2} \text{ and not } \propto D^{-1/2}. \quad (5)$$

3. Large particles ( $r > 150 \text{ \AA}$ ): the yield stress becomes independent of grain size above a certain particle size:

$$\Delta\sigma_b = 0. \quad (6)$$

### 3.2. Electron microscopy

Only the noncoherent  $\epsilon$ -particles can be observed in the electron microscope while the coherent particles are not visible. As long as particles are sheared the electron micrographs show that dislocations are formed at grain boundaries and move through the crystal with small curvature (Fig. 5).

At a mean particle radius of about 30 to 40  $\text{\AA}$  the dislocations start to bypass some of the largest particles. The curvature increases and at still larger particles sizes the emission of new dislocations at particle interfaces was observed (Fig. 6) [3, 8]. These dislocations form at the incoherent portions of the interface. It is likely that this occurs by a similar mechanism as formation at grain boundaries; however, the maximum radius of curvature of the dislocations

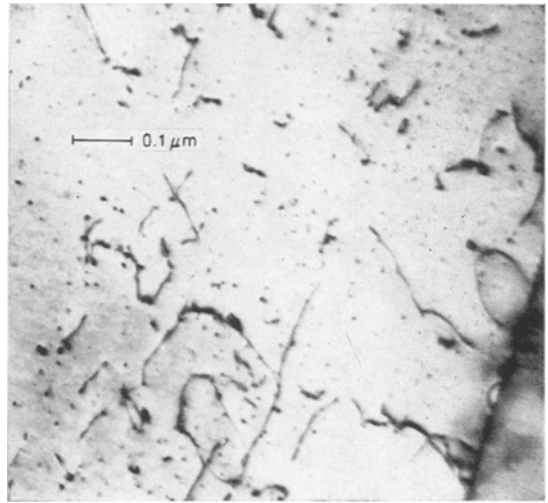


Figure 5 Interaction of particles and dislocations at 0.4% plastic deformation: partial cutting and bypassing. Heat-treatment: 100 h, 500°C.

is limited to that of the particle.

The role of grain boundaries at the beginning of plastic deformation was also observed.

*Condition 1:* Dislocations start to form at grain boundaries (Figs. 5 and 7). These dislocations pile up in the interior of the grain. Both observations are in agreement with the fact that the grain-size dependence follows the Petch-Hall-relationship.

*Condition 2:* In this condition an intermediate behaviour is observed. In a few cases particles act already as dislocation sources and the tendency to form dislocation pile ups is decreased, because dislocations are impeded by larger particles.

*Condition 3:* Dislocations are produced in large numbers by particles. Emission of dislocations at grain boundaries becomes negligible. The dislocations are very evenly distributed in the grains and no pile ups are observed. In this condition the yield stress was independent of grain size.

## 4. Discussion

The experimental results have shown that for the age-hardened conditions at which the particles are sheared an additive behaviour of particle hardening and grain-boundary hardening occurs. This indicates that for these conditions the basis for the application of the Petch-Hall-relationship

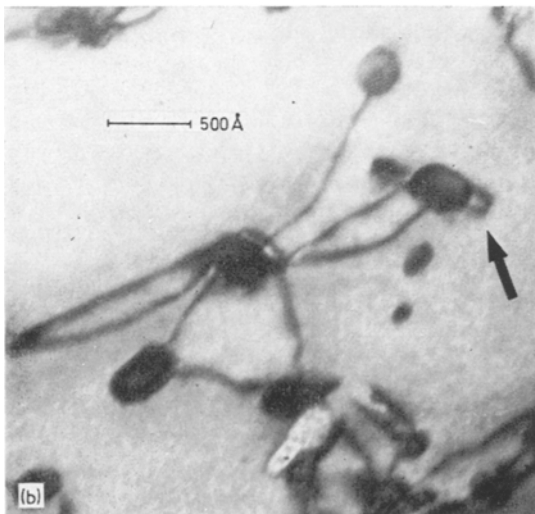
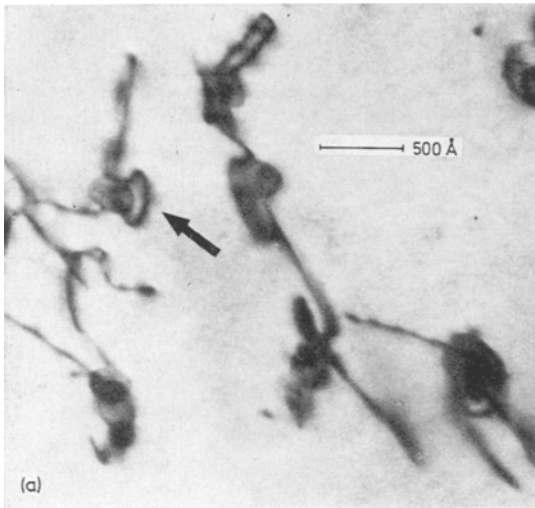


Figure 6 Dislocation loops at large particles at 0.4% plastic deformation. Heat-treatment: 100 h, 600°C.

is unchanged. Contrary to this is the situation for large particles. The independence of yield stress from the grain size indicates that precipitation hardening has led to a qualitative change of the behaviour of the alloy. In order to explain this it is necessary to consider the yield stress not only as a function of grain size but also as a function of dislocation density.

The Petch-Hall-relationship

$$\sigma_y = \sigma_0 + k_y D^{-1/2} \quad (7)$$

gives the amount of grain-boundary hardening if the condition of the grain boundaries and, therefore,  $k_y$  is not changed as a function of

grain size. All other contributions to the yield stress except grain size are contained in  $\sigma_0$ .

There is a defined relationship between grain size,  $D$ , and dislocation density,  $\rho$ . If we consider a constant amount of deformation  $\epsilon_y$  at the yield stress, then it follows that

$$\epsilon_y = b \cdot \rho_y \lambda \quad (8)$$

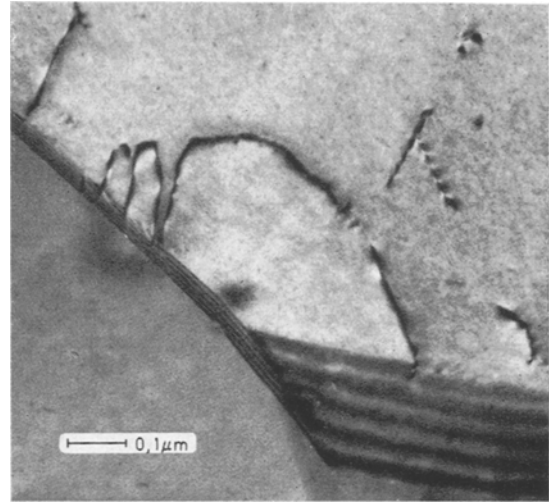


Figure 7 Generation of dislocation loops at a grain boundary at 0.4% plastic deformation. Heat-treatment: 1 h, 500°C.

where  $b$  is the Burgers vector and  $\lambda$  the average path of travel of a dislocation. If this path of travel is equal to the grain size, it follows that

$$\epsilon_y = b \rho_y D \quad (9)$$

On this basis, Equation 7 can be also written as a function of dislocation density which is a function of grain size,  $\rho_y = f(D)$  for a given amount of strain [11]:

$$\sigma_y = \sigma_0 + \alpha G b \rho_y^{1/2} = \sigma_0 + \frac{\alpha \epsilon_y^{1/2} G b^{1/2}}{D^{1/2}} \quad (10)$$

where  $\alpha = 0.5, \dots, 1$  for  $\alpha$ -Fe [12, 13].

Equation 10 indicates that under these conditions the grain-size dependence of Equation 7 still holds.  $k_y$  only contains the plastic strain  $\epsilon_y$  as a variable:  $k_y = \alpha \epsilon_y^{1/2} G b^{1/2}$ .

If we consider the formation and motion of dislocations as a consequence of the applied stress at the yield stress [14], from Equation 10 a value of  $\rho_y$  can be obtained. This is the dislocation density which has formed at the grain

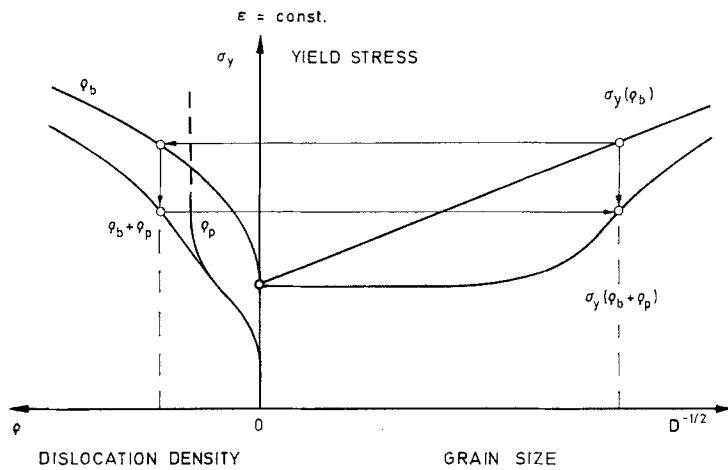


Figure 8 Influence of dislocation density and grain size on the yield stress of an alloy containing two types of dislocation sources.

boundaries and travelled a distance  $D$  at the yield stress  $\sigma_y$ .

$$\rho_y(\sigma_y) = \left( \frac{\sigma_y - \sigma_0}{\alpha G b} \right)^2 = \rho_b \quad (11)$$

In this case it is assumed that no additional dislocation sources are active and that the motion of the dislocations is not impeded between the grain boundaries. If this condition is relaxed, i.e. if dislocations of the density  $\rho_s$  can be formed from additional sources, a second term must be included in Equation 11:

$$\rho_y(\sigma_y') = \left( \frac{\sigma_y' - \sigma_0}{\alpha G b} \right)^2 + \rho_s(\sigma_y') = \rho_b + \rho_s \quad (12)$$

If  $\epsilon_y$  is constant and the path of travel  $D$  is constant, then

$$\rho_y(\sigma_y) = \rho_y(\sigma_y')$$

and

$$\sigma_y' < \sigma_y = \sigma_0 + k_y D^{-1/2} \quad (13)$$

and therefore  $\sigma_y'$  is not proportional to  $D^{-1/2}$ .

Another assumption is that  $\sigma_0$  is not changed due to the additional dislocation sources. It follows from Equation 12 that for a certain grain size the yield stress  $\sigma_y'$  becomes smaller than  $\sigma_y$  due to the additional dislocation sources.

For a quantitative treatment it is necessary to know the number  $\rho_s(\sigma_y')$  of dislocations generated from the additional sources which can be activated at a certain stress. This function is indicated qualitatively in Fig. 8 as  $\rho_p(\sigma_y')$  where particles act as additional dislocation sources.

For our special case it was assumed that at a certain stress only the largest particles are able to produce dislocations. If the external stress is increased further even the smaller particles can become active as dislocation sources. At present no quantitative treatment exists of the emission of dislocations at noncoherent interfaces. The discussion is therefore only possible on a qualitative basis.

We have assumed in Equation 13 that  $\lambda = D$  is constant, if sources additional to the grain boundaries become active. This assumption will not hold in reality. If noncoherent particles are able to produce dislocations the path of travel of the dislocations in the interior of the grain will be increasingly impeded by dislocations which have originated in the same way from other neighbouring particles. This leads to the conclusion that parallel to the increased number of additional sources there will be a decrease in the mean free path of travel of the dislocations. On this basis the discussion of the behaviour of the alloy in the transitional range II is possible. The Petch-Hall-relationship will be valid in the whole range of grain sizes in which the average free path of travel  $\lambda$  is not smaller than the smallest grain size. If, however,  $\lambda$  becomes smaller, a grain-size dependence of yield stress will be expected for all grain sizes which are smaller than  $\lambda$ . For all grain sizes larger than  $\lambda$  the independence of yield stress from grain size will be expected.

Another consequence of the increased number of the additional sources in the interior of the grain and the decrease of the path of travel of the

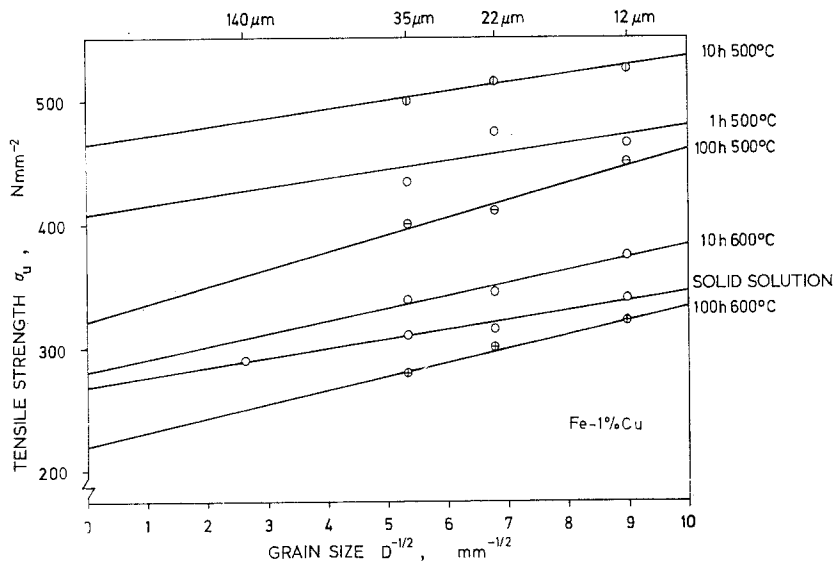


Figure 9 Grain-size dependence of tensile strength in different precipitation conditions.

dislocations is that the yield stress of the alloy can be either decreased as indicated in Equations 12 and 13 or increased if the decrease in the path of travel is dominating. It cannot be decided from the present result which effect is dominant.

Independent of these considerations, the conditions for  $k = 0$  should always follow for the condition that the number of the additional sources is much larger than that of the original grain boundaries and that the path of travel is much smaller than the grain size.

Finally, some additional data from the tensile tests are reported. In Fig. 9 the dependence of tensile strength of grain size is plotted for the ageing conditions mentioned above. It indicates that the independence of grain size of the over-aged alloys is not observed for the tensile strength. An interpretation of these data is difficult because it requires the consideration of the work-hardening behaviour which again varies widely as a function of the ageing condition [8]. The same is valid for the uniform elongation. There was no measurable difference observed at room temperature for the specimen with different grain sizes. The minimum elongation was always observed at an ageing period a little longer than that required to produce maximum yield stress (Fig. 3). An investigation of the fracture behaviour of the alloy as a function of the parameters discussed here and at temperatures below room temperature seems to

be the most useful direction in which this work can be followed.

### Acknowledgements

This work was supported by the Deutsche Forschungsgemeinschaft (DFG). The material was provided by the Hoesch Hüttenwerke AG. We like to express our thanks for this support of this work.

### References

1. D. PECKNER, "The Strengthening of Metals" (Reinhold, London, 1964).
2. E. HORNBOGEN (ed.), "Werkstoffe mit hoher Festigkeit", to be published (Stahl und Eisen, Düsseldorf, 1974).
3. G. STANIEK and E. HORNBOGEN, *Scripta Met.* **7** (1973) 615.
4. E. HORNBOGEN, in "Steel Strengthening Mechanisms" (Climax Molybdenum Cor., Greenwich, Conn., 1970).
5. A. J. E. FOREMAN and M. J. MAKIN, *Canad. J. Physics* **45** (1967) 511.
6. E. HORNBOGEN and R. C. GLENN, *Trans. Met. Soc. AIME* **218** (1960) 1064.
7. H. A. WRIEDT and L. S. DARKEN, *ibid* **218** (1960) 30.
8. E. HORNBOGEN, *Trans. ASM* **57** (1964) 120.
9. E. OROWAN, "Symposium on Internal Stresses in Metals and Alloys" (Institute of Metals, London, 1948) 451.
10. N. J. PETCH, *J. Iron Steel Inst.* **174** (1953) 25.
11. H. CONRAD, in "Reinststoffprobleme", Vol. IV

- (edited by M. Balarin) (Akademie-Verlag, Berlin, 1972) p. 409.
12. A. H. KEH and S. WEISSMAN, "Electron Microscopy and Strength of Crystals", (edited by G. Thomas and J. Washburn) (Wiley, New York, 1963).
13. N. IGATA and S. SETO, Proceedings ICSTIS, *Suppl. Trans. ISIJ*, **11** (1971) 1293.
14. G. BÄRO and E. HORNBÖGEN, "Quantitative Relation between Properties and Microstructure" (edited by D. G. Brandon and A. Rosen) (Israel University Press, Jerusalem, 1969) p. 457.

Received 20 December and accepted 31 December 1973.